Research Square

Preprints are preliminary reports that have not undergone peer review.
They should not be considered conclusive, used to inform clinical practice,
or referenced by the media as validated information.

Study of Anisotropy in a Dark Energy Model with Latest Observations

Manish Yadav
Indira Gandhi Mirpur University
Archana Dixit
archana.ibs.maths@gmail.com

Gurugram University
Pardeep Pardeep
Indira Gandhi Mirpur University
Anirudh Pradhan
GLA University
M. S. Barak
Indira Gandhi Mirpur University

Research Article

Keywords: Dark energy, Anisotropic model, Cosmological parameters, Sign-Switching cosmological model

Posted Date: September 17th, 2026

DOI: https://doi.org/10.21203/rs.3.rs-10906006/v1

License: This work is licensed under a Creative Commons Attribution 4.0 International License.
Read Full License

Additional Declarations: No competing interests reported.

Study of Anisotropy in a Dark Energy Model with Latest Observations

Manish Yadav[1]*, Archana Dixit[2]†, Pardeep[1]‡, Anirudh Pradhan[3]§, M.S. Barak[1]¶

[1]Department of Mathematics,
Indira Gandhi University, Meerpur, Haryana, 122502, India
[2]Department of Mathematics,
Gurugram University, Gurugram, Haryana, 122505, India
[3]Centre for Cosmology, Astrophysics and Space Science,
GLA University, Mathura, Uttar Pradesh, 281406, India

Abstract

Recent high-precision cosmological observations have motivated the exploration of extensions to the ΛCDM model that can simultaneously investigate possible deviations from isotropic cosmic expansion and alleviate persistent observational tensions. In this work, we explore the possibility of anisotropic cosmic expansion within a sign-switching or negative dark energy framework by extending the recently proposed Λ_sCDM model to include a free anisotropy parameter, $\Omega_{\sigma 0}$. In this scenario, the effective cosmological constant dynamically evolves from a negative value in the early universe to a positive value at later times, with the transition occurring at a characteristic redshift $z_\dagger$. We confronted this extended model with the latest cosmological observations, including Planck 2018 CMB measurements, DESI DR2 BAO data, and the PantheonPlus&SH0ES Type Ia supernova sample. From a comprehensive joint likelihood analysis of the CMB, CMB+DR2, and CMB+PP&SH0ES datasets, we found that the present-day anisotropy parameter is tightly constrained to be of the order $\Omega_{\sigma 0} \sim 10^{-16}$ at 95% C.L., indicating a highly suppressed but non-vanishing anisotropic contribution. The transition redshift $z_\dagger$ was also well constrained, exhibiting a robust lower 1σ bound when the BAO data were excluded. Furthermore, the combined CMB+PP&SH0ES dataset yields $H_0 = 72.25 \pm 0.90$ km s^{-1} Mpc^{-1}, strongly favoring the SH0ES calibration, while the standard ΛCDM model remains closer to the CMB-preferred value of $H_0 = 68.69^{+0.31}_{-0.38}$ km s^{-1} Mpc^{-1}. Within our extended framework, the Hubble tension was reduced to approximately the 3.7σ level. Model comparison based on the Akaike Information Criterion (AIC) and Bayesian Information Criterion (BIC) indicates that the Λ_sCDM+$\Omega_{\sigma 0}$ model receives very strong observational support relative to the standard ΛCDM cosmology.

Keywords: Dark energy; Anisotropic model; Cosmological parameters; Sign-Switching cosmological model

1 Introduction

For many years, the scientific community has regarded the standard ΛCDM model as a robust framework that fits both theoretical expectations and a wide range of observational data remarkably well (Riess et al., 1998; Perlmutter et al., 1999; Aghanim et al., 2020; Alam et al., 2021; Abbott et al., 2022; Yadav et al., 2026d). However, in recent years, cosmic tensions have emerged as one of the most debated

*manish.math.rs@igu.ac.in
†archana.ibs.maths@gmail.com
‡pardeep.math.rs@igu.ac.in
§pradhan.anirudh@gmail.com
¶ms_barak@igu.ac.in

topics in modern cosmology—particularly the Hubble tension (Valentino et al., 2021; Yadav et al., 2025b; Chen et al., 2024; Verma et al., 2026; Montani et al., 2026; Valentino et al., 2025) and cosmic expansion anisotropy (Boubel et al., 2025; Kibaroglu & Senay, 2025). These conflicts exist between the direct findings of H_0 from local observations using standard candles and the indirect estimates of H_0 acquired from cosmic model fitting. These discrepancies have spurred the scientific community to pursue alternative explanations, whether by invoking new physical theories (Yadav et al., 2025c) or by examining potential sources of systematic errors in observations.

Here, we explore anisotropic expansion that can be generated after decoupling, which has been suggested as a possible explanation for the low CMB quadrupole. Such scenarios are not considered in this work, because they require anisotropic stresses after decoupling from non-geometric sources, including vector fields or modified gravity theories (Brans–Dicke theory) (Mimoso & Wands, 1995; Akarsu et al., 2020; Campanelli et al., 2007; Koivisto & Mota, 2008; Almeida et al., 2019; Akarsu et al., 2020; Faraoni & Coté, 2018). In tilted cosmological models, anisotropic expansion can also persist late and is explored as a possible explanation for cosmological tensions (H_0 and S_8) and dipole discrepancies. In this study, we focused only on orthogonal (non-tilted) universe models. However, tilted models can lead to very different conclusions and theories, sometimes suggesting modification of the ΛCDM model and reconsideration of the Einstein–de Sitter universe. In these tilted scenarios, observers (such as those in galaxies such as the Milky Way) who are part of a large-scale bulk flow might incorrectly interpret the observations and conclude that the universe is accelerating; however, several studies suggest that the apparent acceleration inferred from Type Ia supernova data disappears when bulk-flow–induced anisotropies are taken into account, a bulk-flow–aligned dipole is identified, whereas the monopole component shows no significant deviation from zero (Colin et al., 2011; Lin et al, 2016; Li et al., 2015; Wilczynska et al., 2020; Migkas et al., 2020; Chang et al., 2018; Secrest et al., 2021; Siewert et al., 2021; Migkas et al., 2021; Rahman et al, 2022; Heinesen & Macpherson , 2022; Park & Ratra, 2019, 2020; Macpherson & Heinesen, 2021; Yeung & Chu, 2022; Krishnan et al., 2022; Luongo et al., 2022; Camarena et al., 2022; Asvesta et al., 2022). These findings have ensured a sustained and recently renewed interest in anisotropic cosmologies.

In modern times, it is worth noting that model-independent analyses place upper bounds on the present-day expansion anisotropy, quantified by $\Omega_{\sigma 0}$, at the level of $\mathcal{O}(10^{-3})$ based on Type Ia supernova observations (Campanelli et al., 2011; Kalus et al., 2013; Wang & Wang, 2018; Jimenez et al., 2015; Soltis et al., 2019; Zhao et al., 2019; Hu et al., 2020; Singh et al., 2025; Singh & Krishnannair, 2026; Singha & Singh, 2026). Similar upper bounds of $\Omega_{\sigma 0}$ lie from $\mathcal{O}(10^{-3})$ to $\mathcal{O}(10^{-5})$ with the Hubble data (containing 46 redshift points) and supernova observations (Bhardwaj et al., 2022). In addition, our forthcoming analysis of an anisotropic cosmological model with bulk viscosity parameterization yielded an upper bound on $\Omega_{\sigma 0}$ of approximately $\mathcal{O}(10^{-4})$, derived using an expanded Hubble data set consisting of 57 redshift points (Dixit et al., 2023). These upper bounds are consistent with model-dependent observational constraints over the range up to redshifts $z \lesssim 2.4$ obtained from $H(z)$ and/or supernova data, within an expansion anisotropy model (Akarsu et al., 2019; Amirhashchi & Amirhashchi, 2020; Singh & Krishnannair, 2026). Recently, the author investigated the simplest anisotropic extension of the ΛCDM model, namely the Bianchi type-I spacetime, using a combined analysis of BAO, BBN, OHD, and PantheonPlus with SH0ES data. This study yielded an upper bound on the present-day expansion anisotropy of order $\mathcal{O}(10^{-14})$ at the 95% confidence level, for all combination datasets(with and without the inclusion of the SH0ES data set)(Yadav, 2023). A similar investigation was carried out in (Yadav et al., 2024), where a dynamical dark energy model was considered, and anisotropy constraints of the same order were obtained using the same combination of observational data. In Ref. (Akarsu et al., 2019), the author integrating higher-redshift data, the constraint $\Omega_{\sigma 0} \lesssim 10^{-3}$ from the amalgamated Pantheon supernova and H(z) data is refined to $\Omega_{\sigma 0} \lesssim 10^{-15}$ through the inclusion of CMB and BAO observations pertinent to $z \sim 1100$, and is further restricted to $\Omega_{\sigma 0} \lesssim 10^{-23}$ to maintain the accurate predictions of standard BBN at $z \sim 10^9$. A related investigation was performed in (Akarsu et al., 2023a), where the author examined both expansion anisotropy and spatial curvature from several cosmic data sets and

reported very small present-day anisotropies. The independent bounds also arise from the observed CMB quadrupole temperature anisotropy, $\Delta T/T \sim 10^{-5}$, implying $\Omega_{\sigma 0} \lesssim 10^{-20}$ and a corresponding anisotropy at recombination of order $\Omega_{\sigma,\mathrm{rec}} \sim 10^{-5}$ at $z_{\mathrm{rec}} \sim 10^{3}$ (Martinez-Gonzalez & Sanz, 1995; Kogut et a., 1997; Barrow, 1997). These already stringent bounds are further strengthened even by the full *Planck* temperature and polarization data, yielding $\Omega_{\sigma 0} \lesssim 10^{-22}$ (Saadeh et al., 2016a,b).

Anisotropic cosmological models have been extensively studied using a wide range of observational probes and within various theoretical frameworks of gravity. These investigations include, for example, Bianchi type I and Bianchi type-V spacetimes in modified gravity theories such as $f(Q)$ (Esposito et al., 2022; Dixit et al., 2022), $f(Q,T)$ (Solanke et al., 2023), $f(T,B)$ (Paliathanasis, 2022) gravity, anisotropic cosmological models with accelerated expansion based on EoS parameters (Mandal, 2026), and holographic dark energy scenarios in locally rotationally symmetric (LRS) Bianchi type-I and III universes (Koussour et al., 2022; Singh, 2023; Mule et al., 2024; Singh et al., 2025). Further studies have explored Bianchi type I cosmologies within the context of bimetric theories of gravitation (Borkar & Charjan, 2010), as well as Bianchi type-I_0 models incorporating holographic dark energy in $f(T)$ gravity (Fayaz et al., 2015). In addition to many other anisotropic scenarios various modified gravity theories and cosmological settings have been proposed and analyzed, highlighting the broad and ongoing interest in anisotropic cosmologies (Palacios-Córdoba et al., 2026; Vinutha & Kavya, 2022; Pradhan et al., 2022; Santhi & Chinnappalanaidu, 2023).

The most widely studied negative dark energy model, inspired by graduated dark energy (Akarsu et al., 2020) is the Λ_{s}CDM model. Compared with the standard cosmological model, it introduces one additional free parameter, the transition redshift $z_\dagger$, and is characterized by a sign-switching cosmological constant Λ_s. This model has been shown to alleviate several long-standing tensions in cosmological observations, including the H_0 tension, the S_8 tension, and so-called M_B tension (Akarsu et al., 2021, 2023c,b), while also benefiting from the high-precision constraints provided by *Planck* data. However, Λ_{s}CDM does not show good agreement with the full set of BAO measurements, although it remains consistent with the Lyman-α forest observations (Akarsu et al., 2021, 2026a). When supernova data are combined with CMB observations, the additional free parameter becomes well constrained (Akarsu et al., 2023c), and the associated cosmological tensions are significantly reduced. The Λ_{s}CDM model is grounded in a physically well-motivated dark energy framework introduced by Akarsu *et al.*, (Akarsu et al., 2020) in which the cosmological constant allows a minimal dynamical evolution governed by a null inertial mass density proportional to the vacuum energy density ($\rho_{inert} \propto \rho^{\lambda} < 0$, where $\lambda < 1$ is a real constant), with a negative cosmological constant in the early universe. In the regime of large negative λ, this construction naturally yields a smooth and spontaneous transition in the sign of Λ, evolving from negative values at high redshifts to positive values at later times. This mechanism can be interpreted as a transition of the cosmic vacuum from an anti-de Sitter phase to a de Sitter phase occurring around redshift $z \simeq 2$, an idea that is well aligned with expectations from string theory and vacuum landscape arguments. Building on this theoretical foundation, the Λ_{s}CDM model has been systematically developed in subsequent studies and has been shown to provide a substantially improved fit to cosmological observations (Yadav et al., 2026a, 2025a; Akarsu et al., 2026b, 2025; Bouhmadi-López & Ibarra-Uriondo, 2025ba,b).

In this study, for the first time, we simultaneously incorporate cosmic expansion anisotropy and negative dark energy of cosmos to investigate their combined impact on cosmological parameter estimation and to assess their potential role in alleviating existing cosmological tensions, which are present in the current universe. We extend the sign-switching dark energy framework (Yadav et al., 2026a) by allowing for anisotropic expansion, thereby going beyond the standard isotropic assumptions of ΛCDM. The proposed extension allows for a comprehensive analysis of late-time cosmological dynamics within a single framework, where both dark energy sign transitions and anisotropic expansion contribute to background evolution. The reminder of the paper is organized as follows. In Section I, we discuss the theoretical background and previous studies related to anisotropic expansion and negative dark energy.

In Section II, we introduce the observational data sets utilized—CMB, DR2, and PP&SH0ES—and explain the methodology adopted for the analysis. Section III presents the main results and their cosmological implications. Section IV summarizes the conclusions drawn from this study.

2 Anisotropic Cosmological Model

In this study, we consider a cosmological background that is spatially homogeneous but anisotropic universe, described by the Bianchi type I spacetime, which generalizes the spatially flat Friedmann–Lemaître–Robertson (FLRW) cosmology by allowing the universe to expand at different rates along three mutually orthogonal spatial directions. The geometry of spacetime in this framework is specified by a diagonal metric with time-dependent scale factors. Accordingly, the line element is expressed as:

$$ds^2 = -dt^2 + l^2(t)\,dx^2 + m^2(t)\,dy^2 + n^2(t)\,dz^2, \tag{1}$$

where $l(t), m(t), n(t)$ denote the directional scale factors along three mutually orthogonal directions, x-, y-, and z-axes, respectively. The gravitational dynamics of the spacetime geometry are governed by Einstein's field equations for general relativity as follows:

$$G_{\mu\nu} \equiv R_{\mu\nu} - \frac{1}{2}g_{\mu\nu}R = 8\pi G T_{\mu\nu}. \tag{2}$$

We consider a perfect-fluid energy–momentum tensor in diagonal form, characterized by isotropic pressure p and energy density ρ, such that$T^{\mu}_{\nu} = \mathrm{diag}(-\rho,\, p,\, p,\, p)$. The field equations for Bianchi type-I described by Eq.1 are expressed as:

$$\frac{\dot{l}\dot{m}}{lm} + \frac{\dot{m}\dot{n}}{mn} + \frac{\dot{l}\dot{n}}{ln} = 8\pi G\rho, \tag{3}$$

$$\frac{\ddot{m}}{m} + \frac{\ddot{n}}{n} + \frac{\dot{m}\dot{n}}{mn} = -8\pi G p, \tag{4}$$

$$\frac{\ddot{l}}{l} + \frac{\ddot{n}}{n} + \frac{\dot{l}\dot{n}}{ln} = -8\pi G p, \tag{5}$$

$$\frac{\ddot{l}}{l} + \frac{\ddot{m}}{m} + \frac{\dot{l}\dot{m}}{lm} = -8\pi G p. \tag{6}$$

The average scale factor and comoving volume are defined as $a(t) = (l * m * n)^{1/3}$ and $V(t) = l * m * n$, respectively, with normalization $V(t_0) = 1$. The directional Hubble parameters $H_x = \frac{\dot{l}}{l}$ - along x-axis , $H_y = \frac{\dot{m}}{m}$ - along the y-axis, and $H_z = \frac{\dot{n}}{n}$ along the z-axis are define as the mean Hubble rate:

$$H = \frac{1}{3}\dot{V}/V = \frac{1}{3}(H_x + H_y + H_z). \tag{7}$$

We quantified anisotropic expansion with the help of shear scalar in directional Hubble parameter terms, read as: $\sigma^2 = \frac{1}{6}\Big[(H_x - H_y)^2 + (H_y - H_z)^2 + (H_z - H_x)^2\Big]$. Substituting of Eq.4, Eq.5, and Eq.6 into Eq.3 allows the field equations to be expressed in an alternative form as follows:

$$3H^2 = 8\pi G(\rho_r + \rho_m + \rho_\Lambda) + \sigma^2, \tag{8}$$

For the radiation, matter, and dark energy components, the energy conservation equation is given by $\dot{\rho} + 3H(\rho + p) = 0$. Radiation and pressure-less matter are described by the EoS $p_r/\rho_r = 1/3$, and $p_m/\rho_m = 0$ respectively, which leads to the scaling $\rho_r \propto a^{-4}$ and $\rho_m = \rho_{m0}(1+z)^3$. Using the relationship between the redshift and scale factor , $1 + z = a_0/a$, these expressions becomes $\rho_r = \rho_{r0}(1+z)^4$ and $\rho_m = \rho_{m0}(1+z)^3$,respectively. By contrast, the cosmological constant satisfies $p_\Lambda = -\rho_\Lambda$, implying a constant energy density $\rho_\Lambda = \text{const.}$. The term σ^2 represents the anisotropy energy density,

which is expressed as $\dot{\sigma} + 3H\sigma = 0$. After integration, we obtain: $\rho_\sigma = \rho_{\sigma 0}(1+z)^6$. For a radiation and dust-filled universe, the dimensionless density parameters are defined as $\Omega_r = \rho_r/\rho_c$, $\Omega_m = \rho_m/\rho_c$ and $\Omega_\sigma = \rho_\sigma/\rho_c$, where the critical density is given by $\rho_c = 3H^2/(8\pi G)$, with $8\pi G \simeq 1$. Consequently, the Friedmann equation can be expressed as:

$$H^2 = H_0^2 \left[(1+z)^4\Omega_{r0} + (1+z)^3\Omega_{m0} + \Omega_{\Lambda 0} + (1+z)^6\Omega_{\sigma 0}\right]. \tag{9}$$

The current CMB observations of the anisotropy density parameter $\Omega_\sigma = \sigma^2/(3H^2)$ to constrain $\Omega_{\sigma 0} \lesssim 10^{-18}$, indicating that any primordial anisotropy must be extremely small at present. Nevertheless, in early epochs the shear term can significantly modify the expansion history, while at later times the cosmological constant drives the universe toward isotropy, smoothly recovering the standard ΛCDM limit as $\sigma \to 0$. Eq.9 represents a spatially flat, homogeneous but anisotropic extension of the standard ΛCDM cosmology.

In this framework, we modify Friedmann's Eq.9 by replacing the standard dark-energy density associated with the cosmological constant with a sign-switching vacuum energy density, $\Lambda \longrightarrow \Lambda_{\rm s} \equiv \Lambda_{\rm s0}, {\rm sgn}(z_\dagger - z)$ (Yadav et al., 2026a), where $\Lambda_{\rm s0} > 0$ corresponds to the present-day value of the cosmological term, $z_\dagger$ denotes the redshift at which the sign transition occurs, and ${\rm sgn}(x)$ is the usual signum function. Thus, for $z > z_\dagger$ (the early universe), the model predicts an AdS-like phase with $\Lambda_{\rm s} < 0$, whereas for $z < z_\dagger$, the vacuum energy becomes positive, leading to the observed late-time acceleration.

Consequently, the background dynamics in the presence of anisotropy and a sign-switching vacuum energy $\Lambda_{\rm s}$CDM+$\Omega_{\sigma 0}$ are governed by a modified Friedmann equation of the form:

$$\frac{H^2(z)}{H_0^2} = \Omega_{\sigma 0}(1+z)^6 + \Omega_{r0}(1+z)^4 + \Omega_{m0}(1+z)^3 + \Omega_{\Lambda_{\rm s0}}{\rm sgn}(z_\dagger - z), \tag{10}$$

where Ω_{σ_0},Ω_{r0}, Ω_{m0}, and $\Omega_{\Lambda_{\rm s0}}$ are the current density parameters of anisotropy, matter, and sign-switching vacuum component, respectively. These parameters satisfy the normalization condition, in which their sum equals unity.

3 Datasets and methodology

Cosmic Microwave Background (CMB): In this study, we adopted a highly reliable legacy CMB dataset. It includes detailed measurements of the polarization power spectra and temperature anisotropies, lensing reconstructions and their cross-spectra,(Aghanim et al., 2020; Ade et al., 2016),viz., the high-ℓ `Plik` likelihood for the ($30 \leq \ell \leq 1996$) TE and EE as well as for ($30 \leq \ell \leq 2508$) TT, the low-ℓ ($2 \leq \ell \leq 29$) EE-only likelihood based on the `SimAll` method, as well as measurements of the CMB lensing, the low-ℓ ($2 \leq \ell \leq 29$) EE-only TT-only likelihood from `Commander` component-separation algorithm.

Dark Energy Spectroscopic Instrument Data Release 2 (DR2): The DESI DR2 BAO measurements use several tracers, including luminous red galaxies, bright galaxies, quasars, emission line galaxies, and the Lyman-α forest. The observation are provided in terms of the transverse comoving distance D_M/r_d, angle-averaged distance D_V/r_d, and Hubble distance D_H/r_d, where r_d denotes the comoving sound horizon at the drag epoch. The specific measurements adopted in this analysis are listed in Table IV in Ref. (Abdul Karim et al., 2025; Yadav et al., 2026b).

Pantheon+SH0ES (PP&SH0ES): We use the PantheonPlus compilation of 1550 spectroscopically confirmed Type Ia supernovae from 18 diffrent surveys spanning the redshift range $0.01 < z < 2.26$ (Scolnic et al., 2022), with absolute magnitudes calibrated using Cepheid host distance measurements (Riess et al., 2022; Yadav et al., 2026c).

In this work, we employ the Boltzmann CLASS code (Brinckmann & Lesgourgues, 2019) together with the Bayesian analysis framework `MontePython` (Audren et al., 2013) to derive cosmological constraints

using the Markov Chain Monte Carlo (MCMC) technique. We aimed to explore the sign switch dark energy model with expansion anisotrop (Λ_sCDM+$\Omega_{\sigma 0}$). The MCMC chain results were analyzed within GetDist (Lewis, 2019), and the convergence of the chains was ensured by applying the Gelman–Rubin criterion (Gelman & Rubin, 1992), requiring $R-1 \leq 0.01$. For each parameter constraint, we ran four independent chains with 100,000 steps, discarding the first 30,000 steps as burn-it. We adopted uniform priors on the cosmological parameters as follows: $\Omega_b h^2 \in [0.005, 0.1]$, $\Omega_c h^2 \in [0.001, 0.99]$, $100\,\theta_s \in [1.03, 1.05]$, $\ln(10^{10} A_s) \in [3.0, 3.18]$, $n_s \in [0.9, 1.1]$, and $\tau_{\rm reio} \in [0.04, 0.125]$ $z_\dagger \in [1, 3]$ and $\Omega_{\sigma 0} \in [0, 0.1]$ for Λ_sCDM+$\Omega_{\sigma 0}$ model.

4 Results and discussions

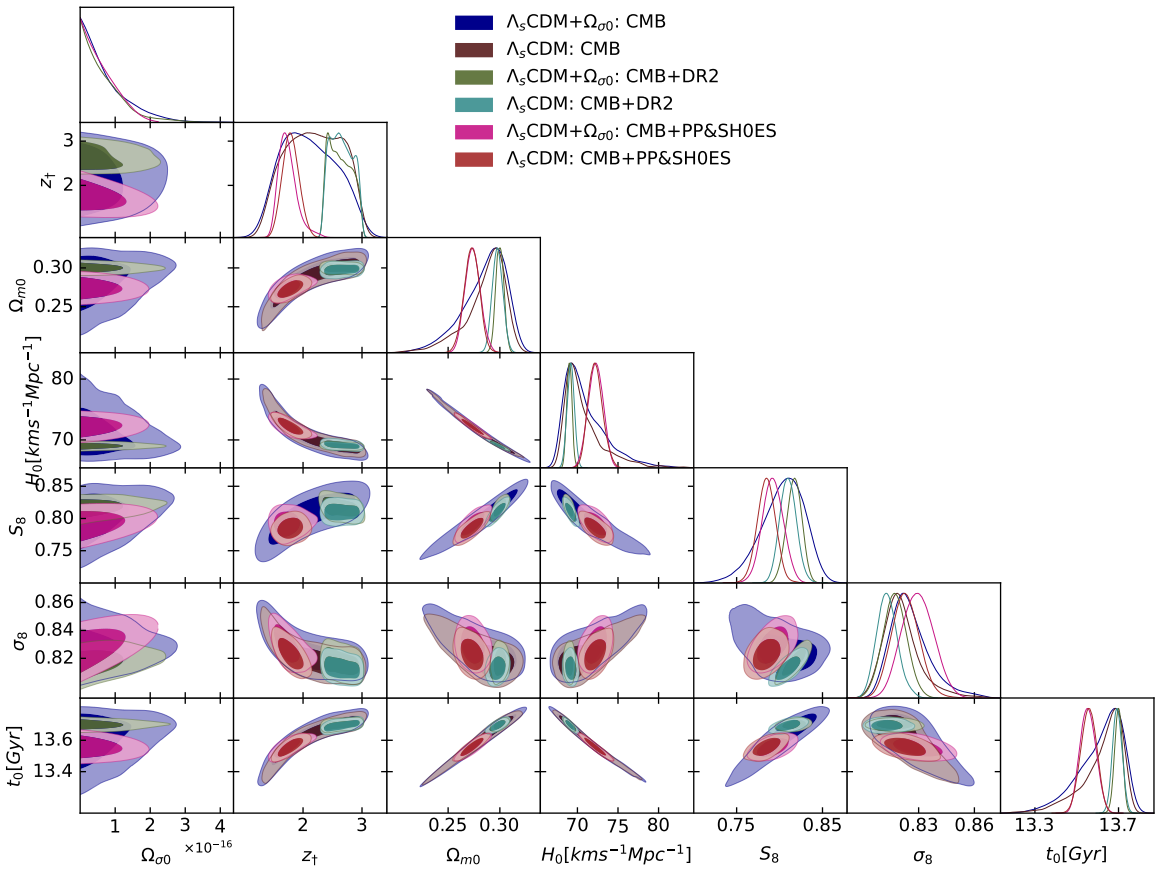


Figure 1: The 1D and 2D marginalized confidence intervals (68% and 95%) for different cosmological parameters constrained by CMB, CMB+DR2, and CMB+DR2+PP&SH0ES within Λ_sCDM+$\Omega_{\sigma 0}$ framework.

Table 1 presents the constraints on the cosmological parameters (baseline and derived parameters) at 68% and 95% C.L for the Λ_sCDM+$\Omega_{\sigma 0}$, Λ_sCDM and ΛCDM models, obtained from high- and low-redshift independent cosmological dataset combinations such as CMB, CMB+DR2, and CMB+PP&SH0ES. In Fig.1, we display the 1D and 2D confidence regions (68% and 95%) for the anisotropic Λ_sCDM+$\Omega_{\sigma 0}$ and Λ_sCDM sign-switch models based on the joint dataset combination. In both cases (Table.1 and Fig.1), the upper limit on the anisotropy parameter obtained from the CMB-only dataset was constrained to $\Omega_{\sigma 0} < 0.74 \times 10^{-16}$ at 95% C.L. One can visualize that the same order of magnitude of anisotropic expansion is presented in Table.1 for the other two combinations of datasets; however, the mean value of the anisotropy parameter shows a slight variation for the CMB+DR2 and CMB+PP&SH0ES dataset combinations. This derived order of magnitude closely matches that

Ref.(Amirhashchi, 2018; Amirhashchi & Amirhashchi, 2019). Moreover, such a level of expansion anisotropy in the present universe within the sign-switch anisotropic model is consistent with results reported in other studies (Akarsu et al., 2019, 2023a). We notice that the anisotropic component is tightly constrained by CMB observations, with $\Omega_\sigma/\Omega_r \sim 10^{-6}$ at $z \sim 1100$, and it dilutes faster than radiation ($\propto a^{-6}$), becoming negligible at late times. Therefore, its impact on low-redshift probes such as DR2 and PP&SH0ES is minimal. The observed improvement in the fit is primarily driven by the sign-switching cosmological model, while the anisotropic contribution remains subdominant and should be interpreted with caution. Adding DR2 or PP&SH0ES to the CMB-only dataset significantly improves the constraints on the anisotropy parameters by reducing their correlations with other cosmological parameters as shown in Fig.1.

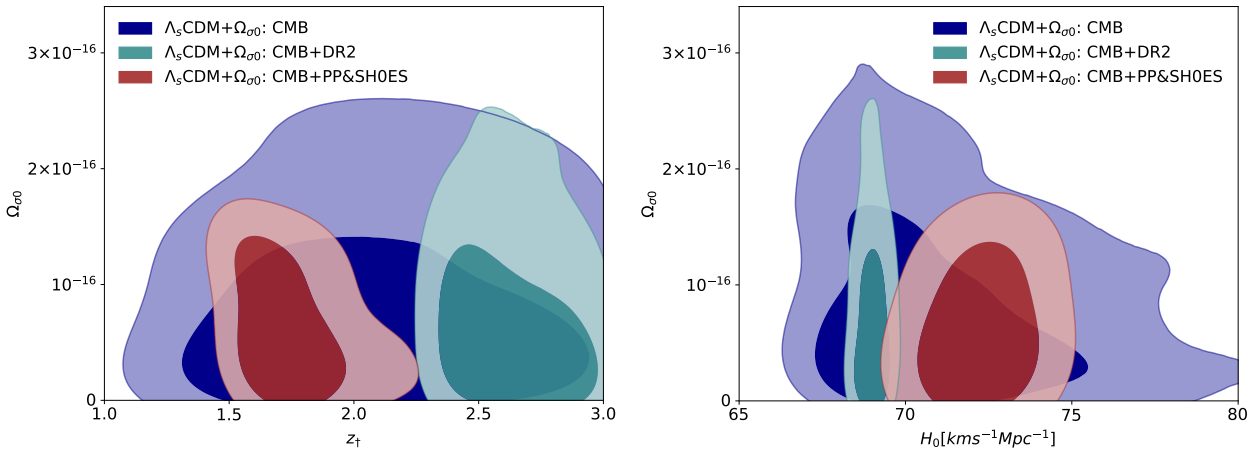


Figure 2: The 2D marginalized confidence regions (68% and 95% C.L.) for the $\Omega_{\sigma 0}$–$z_\dagger$ (Left pannel) and $\Omega_{\sigma 0}$–H_0 (Right pannel) parameter planes derived from CMB, CMB+DR2, and CMB+DR2+PP&SH0ES datasets within the Λ_sCDM+$\Omega_{\sigma 0}$ framework.

As shown in Fig.2 (left panel), the CMB-only data indicated no strong statistical correlation between $\Omega_{\sigma 0}$ and $z_\dagger$. When the DR2 datasets are included with CMB, the 95% contour region of the $\Omega_{\sigma 0}$–$z_\dagger$ plane becomes significantly tighter and largely falls within the 68% contour region of the CMB-only analysis and a similar trend is observed for the CMB+PP&SH0ES combination. From the 1D marginalized distribution of $z_\dagger$ in Fig.1, we find that only a lower bound is obtained, whereas no upper bound is well constrained using CMB-only data from both sign-switch models. However, after adding the DR2 dataset to CMB, the distribution exhibited a sharper peak with a well-defined lower bound, and the mean value of $z_\dagger$ shifted toward higher values at the 95% C.L from Λ_sCDM+$\Omega_{\sigma 0}$ model, meanwhile, in the sign-switch Λ_sCDM model without anisotropy, we also obtain $z_\dagger > 2.36$ at 95% C.L. from the CMB+DR2 dataset combination. Therefore, we can conclude that the inclusion of anisotropy has only a small effect in shifting the mean value of $z_\dagger$ toward higher values from CMB and CMB+DR2 data sets, as can also be seen from the results presented in Table 1. We observe a trend consistent with earlier studies, where the full BAO dataset fails to tightly constrain $z_\dagger$ within the sign-switch model, especially at low redshift (Akarsu et al., 2020). However, the use of Ly-α BAO measurements resulted in comparatively stronger constraints than the full BAO sample (Akarsu et al., 2023c). Due to this, we use without DR2 combination (CMB+PP&PPSH0ES), the average value of $z_\dagger = 1.74$ is tightly constrained, with a well-defined lower 1σ uncertainty, as seen in the 1D marginalized posterior shown in Fig.1, which exhibits both lower and upper bounds. Moreover, the Λ_sCDM model yields nearly identical constraints on $z_\dagger$ as summarized in Table.1. Fig.2 (right panel) presents the 2D marginalized contours, clearly indicating that $\Omega_{\sigma 0}$ and H_0 are well constrained by the observational data combinations considered.

Fig.3 shows the evolution of $H(z)/(1+z)$ verse z for the ΛCDM, Λ_sCDM, and anisotropic Λ_sCDM+$\Omega_{\sigma 0}$ models. At low redshift (late-time universe), both SSDE models gradually converge to the ΛCDM model

Dataset	CMB	CMB+DR2	CMB+PP&SH0ES
Model	Λ_s**CDM**+$\Omega_{\sigma 0}$	Λ_s**CDM**+$\Omega_{\sigma 0}$	Λ_s**CDM**+$\Omega_{\sigma 0}$
	Λ_s**CDM**	Λ_s**CDM**	Λ_s**CDM**
	Λ**CDM**	Λ**CDM**	Λ**CDM**
$10^2\omega_b$	2.250 ± 0.016	2.239 ± 0.013	2.240 ± 0.014
	2.238 ± 0.013	2.253 ± 0.012	2.261 ± 0.013
	2.241 ± 0.015	2.243 ± 0.013	2.245 ± 0.014
$\omega_{\rm cdm}$	$0.1199^{+0.0014}_{-0.0012}$	0.1198 ± 0.0008	0.1197 ± 0.0012
	0.1195 ± 0.0012	0.1194 ± 0.0009	$0.1191^{+0.0011}_{-0.0009}$
	0.1201 ± 0.0012	0.11768 ± 0.00065	$0.1173^{+0.0009}_{-0.0008}$
$100\theta_s$	$1.04026^{+0.00097}_{-0.00071}$	1.04041 ± 0.00077	1.04043 ± 0.00072
	1.04189 ± 0.00029	1.04193 ± 0.00028	1.04195 ± 0.00029
	$1.04192^{+0.00027}_{-0.00031}$	1.04211 ± 0.00028	1.04223 ± 0.00029
$\ln(10^{10}A_s)$	3.040 ± 0.015	3.044 ± 0.014	3.039 ± 0.015
	3.040 ± 0.014	3.042 ± 0.013	3.037 ± 0.014
	3.046 ± 0.014	3.051 ± 0.015	$3.073^{+0.013}_{-0.019}$
n_s	$0.9644^{+0.0045}_{-0.0052}$	0.9646 ± 0.0036	$0.9652^{+0.0048}_{-0.0043}$
	0.9669 ± 0.0043	0.9670 ± 0.0034	$0.9678^{+0.0037}_{-0.0043}$
	0.9656 ± 0.0042	0.9707 ± 0.0033	0.9722 ± 0.0029
$\tau_{\rm reio}$	0.0533 ± 0.0078	0.0548 ± 0.0073	0.0525 ± 0.0076
	0.0528 ± 0.0073	0.0543 ± 0.0064	0.0518 ± 0.0072
	0.0549 ± 0.0072	$0.0601^{+0.0067}_{-0.0079}$	$0.0695^{+0.0094}_{-0.0110}$
$z_\dagger$	> 2.11 (95% CL)	> 2.63 (95% CL)	$1.74^{+0.11}_{-0.18}$
	> 1.45(95% CL)	> 2.36(95% CL)	1.79 ± 0.14
$\Omega_{\sigma 0}$	$< 0.74 \times 10^{-16}$(95% CL)	$< 0.67 \times 10^{-16}$(95% CL)	$< 0.60 \times 10^{-16}$(95% CL)
H_0 [km/s/Mpc]	$70.9^{+1.20}_{-3.10}$	69.02 ± 0.31	72.25 ± 0.90
	$70.77^{+0.79}_{-2.70}$	69.17 ± 0.44	$72.22^{+0.79}_{-0.98}$
	67.40 ± 0.54	68.43 ± 0.29	$68.69^{+0.31}_{-0.38}$
M_B [mag]	–	–	-19.304 ± 0.024
	–	–	$-19.305^{+0.021}_{-0.026}$
	–	–	$-19.401^{+0.009}_{-0.011}$
Ω_m	$0.285^{+0.026}_{-0.013}$	0.300 ± 0.004	0.274 ± 0.007
	$0.286^{+0.023}_{-0.001}$	0.2977 ± 0.0050	0.272 ± 0.007
	0.315 ± 0.008	0.3008 ± 0.0037	$0.298^{+0.005}_{-0.004}$
σ_8	$0.825^{+0.007}_{-0.012}$	0.817 ± 0.006	0.829 ± 0.008
	$0.821^{+0.006}_{-0.011}$	$0.813^{+0.005}_{-0.006}$	0.823 ± 0.007
	$0.812^{+0.006}_{-0.006}$	0.8066 ± 0.0060	0.815 ± 0.006
S_8	$0.804^{+0.028}_{-0.020}$	0.817 ± 0.009	0.792 ± 0.012
	$0.801^{+0.026}_{-0.016}$	0.810 ± 0.010	0.785 ± 0.011
	0.832 ± 0.013	0.8076 ± 0.0083	0.812 ± 0.011
t_0 [Gyr]	$13.62^{+0.13}_{-0.06}$	13.70 ± 0.02	13.55 ± 0.04
	$13.62^{+0.12}_{-0.04}$	13.69 ± 0.02	13.56 ± 0.04
	13.79 ± 0.02	13.76 ± 0.02	13.75 ± 0.02

Table 1: Marginalized constraints (at 68% and 95% CL with uncertainties) on the cosmology parameters of the Λ_sCDM+$\Omega_{\sigma 0}$ and ΛCDM models for different dataset combinations.

for the CMB+DR2 dataset, and the 2D curves of all three models nearly overlap, indicating that the effects of SSDE and anisotropies are negligible at the present epoch. Similarly, at high redshift (early universe), the three models again converge and become almost indistinguishable. However, a noticeable deviation appears in the intermediate redshift region $1 < z < 3$ around the transition epoch, where the sign-switching of the dark energy occurs. In this transition phase, the 2D-trajectories of the SSDE models depart from the ΛCDM model, demonstrating that the sign-switching mechanism significantly

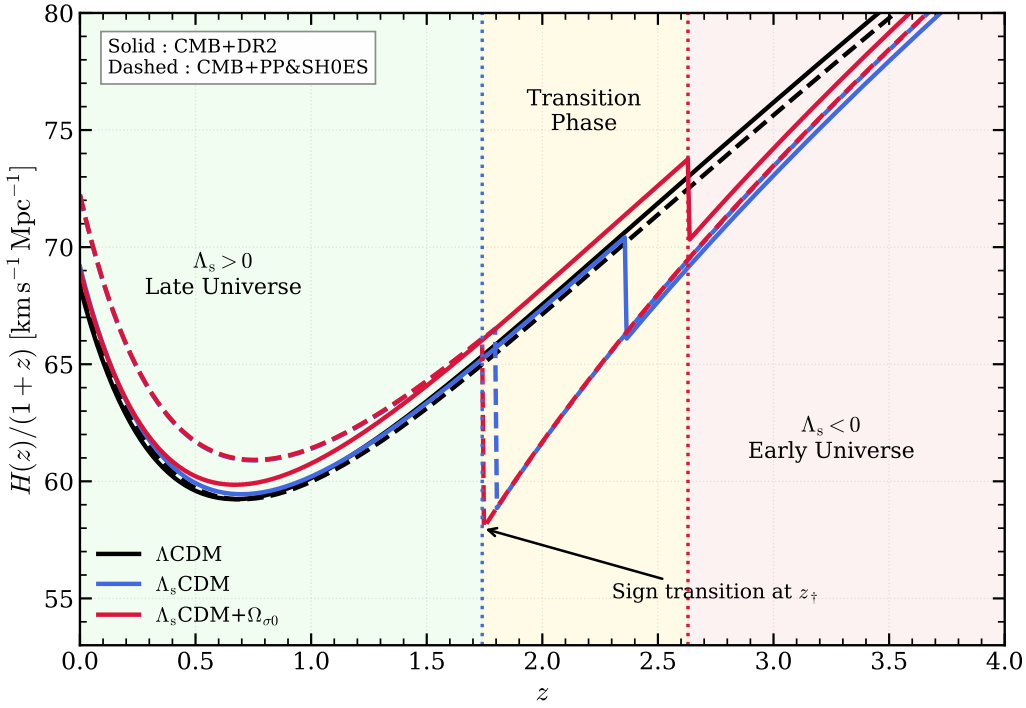


Figure 3: Evolution of the normalized Hubble parameter $H(z)/(1+z)$ for the ΛCDM, Λ_sCDM, and Λ_sCDM+$\Omega_{\sigma 0}$ models constrained by the CMB+DR2 and CMB+PP&SH0ES datasets.

modifies the expansion history.

The long-standing discrepancy between the early-universe (CMB) and late-universe (distance-ladder) measurements of the Hubble constant represents one of the most serious tensions confronting the standard cosmological model. Early-Universe probes within the ΛCDM framework favor $H_0 = 67.40 \pm 0.50$ km s^{-1} Mpc^{-1} from CMB observations (Aghanim et al., 2020). The combined analysis of data from the South Pole Telescope (SPT) and the Atacama Cosmology Telescope (ACT) yields $H_0 = 66.59 \pm 0.46$ km s^{-1} Mpc^{-1} within ΛCDM framework (Camphuis et al., 2025). In contrast, the independent distance-ladder approach, anchored by Cepheid variables and calibrated Type Ia supernovae from SH0ES, gives $H_0 = 73.04 \pm 1.04$ km s^{-1} Mpc^{-1} (Riess et al., 2022), establishing a tension greater than 5σ. The updated SH0ES analysis, strengthened by the inclusion of a new geometric distance anchor, reports $H_0 = 73.17 \pm 0.86$ km s^{-1} Mpc^{-1} (Breuval et al., 2024). When compared with the recent SPT+ACT CMB determination, the statistical significance of the discrepancy increased to above 6.7σ. This persistent tension is consistently observed across different research groups, calibration techniques, Hubble-flow samples, and independent CMB analyses probing various angular scales. In this study, we investigated the constraints on H_0 obtained from both models using all the dataset combinations. From Table 1, we find that by using the CMB data alone, both sign-switch models constrains the Hubble constant to $H_0 = 70.9^{+1.20}_{-3.10}$ km s^{-1} Mpc^{-1} and $H_0 = 70.77^{+0.79}_{-2.70}$ km s^{-1} Mpc^{-1} for Λ_sCDM+Ω_{σ_0} and Λ_sCDM, respectively, whereas the standard ΛCDM model yields $H_0 = 67.40 \pm 0.54$ km s^{-1} Mpc^{-1}. This indicates that both sign-switch models prefer the same higher central value with comparatively larger uncertainty. Moreover, the 1σ uncertainty in the Λ_sCDM model is slightly smaller than that of the extended sign-switch anisotropic Λ_sCDM+Ω_{σ_0} model. When DR2 data are included in the CMB analysis, All three models constrains nearly consistent results, giving $H_0 = 69.02 \pm 0.31$ km s^{-1} Mpc^{-1} for Λ_sCDM+Ω_{σ_0} model, $H_0 = 69.17 \pm 0.44$ km s^{-1} Mpc^{-1} for Λ_sCDM and $H_0 = 68.43 \pm 0.29$ km s^{-1} Mpc^{-1} in the standard model. However, for the datasets combination excluding DR2 and including supernova samples (CMB+PP&SH0ES), our analysis shows that the H_0 constraints obtained from both sign-switch models strongly favoring the SH0ES calibration (Riess et al., 2022), while the standard model remains

closer to the CMB-preferred value at $H_0 = 68.69^{+0.31}_{-0.38}$ km s^{-1} Mpc^{-1}. These results demonstrate that our model provides a better fit to late-time observations and significantly alleviates the Hubble tension, reducing it to approximately the 3.7σ level compared with the standard ΛCDM framework.

Another issue that has garnered significant attention in recent years is the S_8 discrepancy within the standard model, which is linked to measurements of the amplitude of matter clustering. The quantity is expressed as $S_8 \equiv \sigma_8\sqrt{\Omega_m/0.3}$, where Ω_m represents the matter density parameter and σ_8 denotes the fluctuation amplitude at $8\,h^{-1}$ Mpc scales. Under the assumptions of the ΛCDM framework, Planck CMB observations indicate a higher matter clustering amplitude of $S_8 \approx 0.83$ (Aghanim et al., 2020). In contrast, weak lensing surveys such as KiDS, DES-Y3, and HSC suggest lower values around $S_8 \approx 0.76$ (Amon et al., 2022; Asgari et al., 2021; Dalal et al., 2023), leading to a tension of approximately $2-3\sigma$. This discrepancy is somewhat alleviated when the DES-Y3 and KiDS-1000 data are integrated, resulting in a joint constraint of $S_8 \approx 0.79$ (Abbott et al., 2023). Recently, KiDS-Legacy analysis reported $S_8 = 0.815$ (Wright et al., 2025), demonstrating strong consistency with Planck and decreasing the tension to 0.73σ. In this study, we derive almost the same constraint on the S_8 parameter for both sign-switch models, based solely on the CMB dataset, and present it in Table 1, which aligns with recent findings from the KiDS-Legacy results. In contrast, the ΛCDM model constrains a higher mean value of $S_8 = 0.832 \pm 0.013$ for the same dataset. We recently released the DR2 data in conjunction with CMB, and subsequently identified approximate mean constraints of $S_8 = 0.817 \pm 0.009$, $S_8 = 0.810 \pm 0.010$ and $S_8 = 0.808 \pm 0.008$ for $\Lambda_{\rm s}$CDM $+\Omega_{\sigma_0}$ $\Lambda_{\rm s}$CDM and ΛCDM models, respectively, under consideration. Upon further analysis of all three cosmological models derived from the PK18+PP&SH0ES datasets, we observe that the mean constraints on S_8 parameter differed slightly, as presented in Table 1. The constraints on S_8 obtained for three models across all dataset combinations demonstrated alignment with the KiDS-Legacy measurements (Abbott et al., 2023; Wright et al., 2025). To investigate the effect of anisotropy on the S_8 parameter, we compare the first two sign-switch models. Our findings show that the extended anisotropic model ($\Lambda_{\rm s}$CDM+Ω_{σ_0}) does not lead to any significant improvement or noticeable impact on the S_8 constraints compared to the isotropic $\Lambda_{\rm s}$CDM model, indicating that anisotropy has no substantial effect on the S_8 parameter within the sign-switch cosmological framework.

Fig.4 compares the theoretical BAO distance predictions of the ΛCDM model and the two SSDE models ($\Lambda_{\rm s}$CDM and anisotropic $\Lambda_{\rm s}$CDM+$\Omega_{\sigma 0}$) with the observed DR2 measurements. Since the DR2 dataset alone provides relatively weak constraints, we combine it with the CMB data and present the corresponding best-fit predictions for the three BAO distance observables, D_H, D_M, and D_V. We find that the theoretical distance predictions of the ΛCDM and $\Lambda_{\rm s}$CDM models are nearly indistinguishable over the entire redshift range shown in Fig.4, indicating that the sign-switching model without anisotropy remains consistent with the standard ΛCDM model. In contrast, the anisotropic $\Lambda_{\rm s}$CDM+$\Omega_{\sigma 0}$ model exhibits small but systematic deviations from the ΛCDM prediction, reflecting the contribution of the anisotropic component to the evolution of the BAO distance observables. We can see in Fig.4 that the $\Lambda_{\rm s}$CDM+$\Omega_{\sigma 0}$ model provides a better fit than the ΛCDM model for three DR2 measurements based on the physical comoving distance, namely the $D_H/(r_d z^{-2/3})$ data points at $z = 1.48$ and $z = 2.33$, and the $D_M/(r_d z^{2/3})$ data point at $z = 0.95$. For the remaining DR2 measurements, the predictions of the anisotropic $\Lambda_{\rm s}$CDM+$\Omega_{\sigma 0}$ model remain broadly consistent with the observed physical distance measurements. However, they do not exhibit a noticeable improvement over the ΛCDM model.

A natural question concerns the comparative performance of these models relative to that of the standard ΛCDM framework. To quantitatively assess their statistical efficiency, we employ two widely used information-theoretic model selection criteria: the Akaike Information Criterion (AIC) (Akaike, 1974) and Bayesian Information Criterion (BIC) (Schwarz, 1978). These criteria provide a balance between the goodness of fit and model complexity by penalizing the inclusion of additional free parameters, which is define as

$$\mathrm{AIC} = \chi^2_{min} + 2d, \tag{11}$$

$$\mathrm{BIC} = \chi^2_{min} + d\ln N, \tag{12}$$

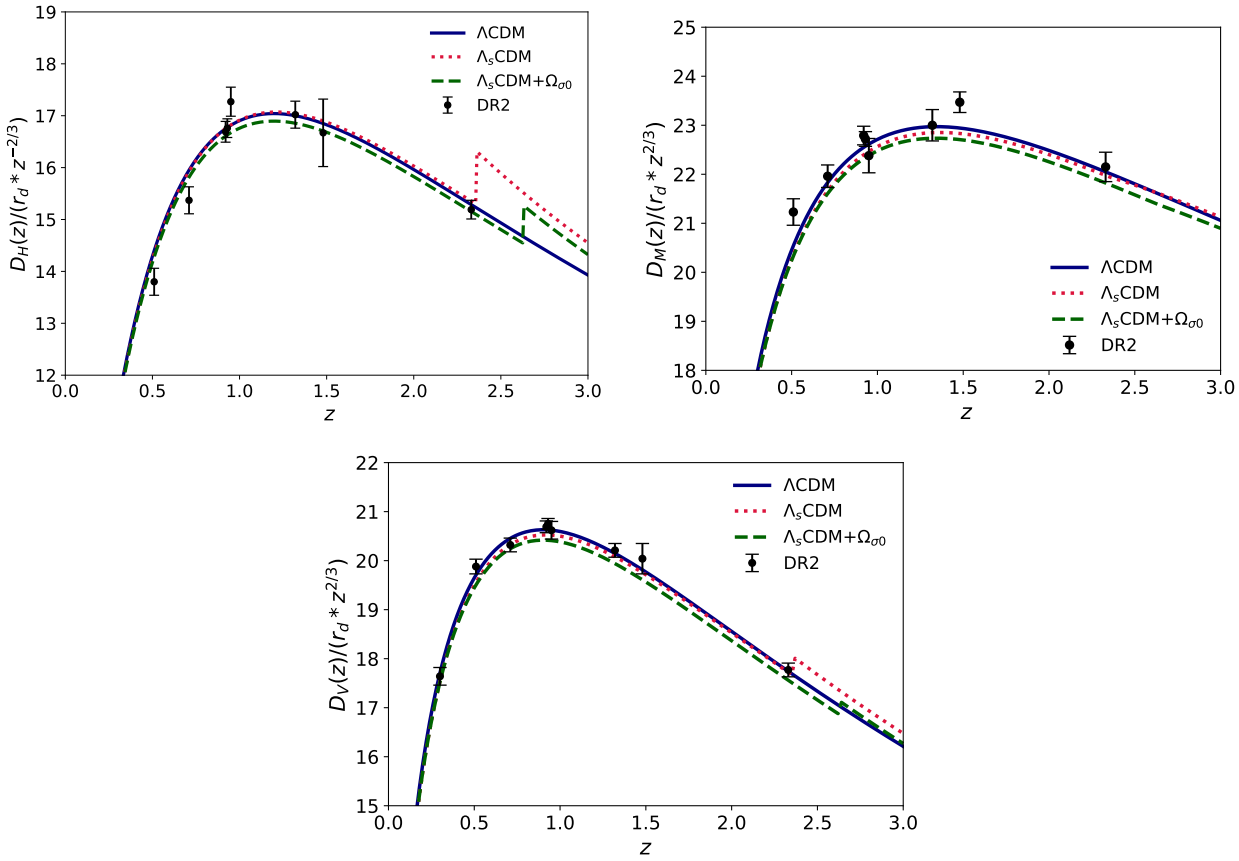


Figure 4: Residuals of $D_H(z)/(r_d * z^{-2/3})$, $D_M(z)/(r_d * z^{2/3})$, and $D_V(z)/(r_d * z^{2/3})$ for the best-fit ΛCDM, Λ_sCDM, and anisotropic Λ_sCDM+$\Omega_{\sigma 0}$ models constrained from CMB+DR2 dataset.

where $\chi^2_{\rm min}$ denotes the minimum chi-square value corresponding to the best-fit parameters, d represents the total number of free parameters in the model, and N is the number of data points used in the analysis. Fig.5 presents a statistical comparison of both SSDE models with the reference ΛCDM model based on ΔAIC and ΔBIC values.

Table 2 presents the AIC and BIC values, along with the corresponding $\chi^2_{\rm min}$ values for all models across the three different dataset combinations. We use these statistical indicators to determine which model provides a better fit to the data.

For the CMB-only dataset, we obtained ΔAIC = 3.98, which is approximately 4 and falls within the range $4 \leq \Delta{\rm AIC} \leq 7$, indicating moderate evidence in favor of standard model relative to the Λ_sCDM+Ω_{σ_0} model. Meanwhile, the Λ_sCDM model are statistically comparable with standard model. This conclusion is further supported by ΔBIC, which indicates a strong statistical distinction, again favoring the ΛCDM model over the sign-switch model, due to its lower BIC value. For the CMB+DR2 combination,ΔAIC, which lies within $0 \leq \Delta{\rm AIC} \leq 2$, suggesting that all three models receive observational support and are statistically comparable. However, the corresponding ΔBIC for the sign-switch model indicates a strong or moderate distinction, favoring the ΛCDM model due to the stronger penalty on additional parameters. When combining CMB with PP&SH0ES data, we observed a significant change, with ΔAIC. This large difference indicates a very strong statistical preference for both sign-switch model over the standard ΛCDM framework. The corresponding ΔBIC indicates a moderate/strong level of distinction, again favoring the Λ_sCDM+Ω_{σ_0}/Λ_sCDM model.

We note that the relatively large values of both ΔAIC and ΔBIC arise from the substantial number

Dataset	CMB	CMB+DR2	CMB+PP&SH0ES
Model	Λ_s**CDM**+$\Omega_{\sigma 0}$	Λ_s**CDM**+$\Omega_{\sigma 0}$	Λ_s**CDM**+$\Omega_{\sigma 0}$
	$\Lambda_{\rm s}$**CDM**	$\Lambda_{\rm s}$**CDM**	$\Lambda_{\rm s}$**CDM**
	ΛCDM	**ΛCDM**	**ΛCDM**
AIC	2796.50	2806.30	4098.80
	2793.06	2806.72	4097.46
	2792.52	2806.78	4117.84
ΔAIC	3.98	−0.48	−19.04
	0.54	−0.06	−20.38
BIC	2850.63	2860.50	4154.86
	2840.51	2851.76	4145.13
	2833.16	2847.43	4159.89
ΔBIC	17.47	13.07	−5.03
	7.35	4.33	−14.76
$\chi^2_{\rm min}$	2780.50	2790.30	4082.80
	2779.06	2792.72	4083.46
	2780.52	2794.78	4105.84

Table 2: The difference, $\Delta\text{AIC} = \text{AIC}_{\rm model} - \text{AIC}_{\Lambda\text{CDM}}$ and $\Delta\text{BIC} = \text{BIC}_{\rm model} - \text{BIC}_{\Lambda\text{CDM}}$ for our model with respect to ΛCDM from all considered data sets.

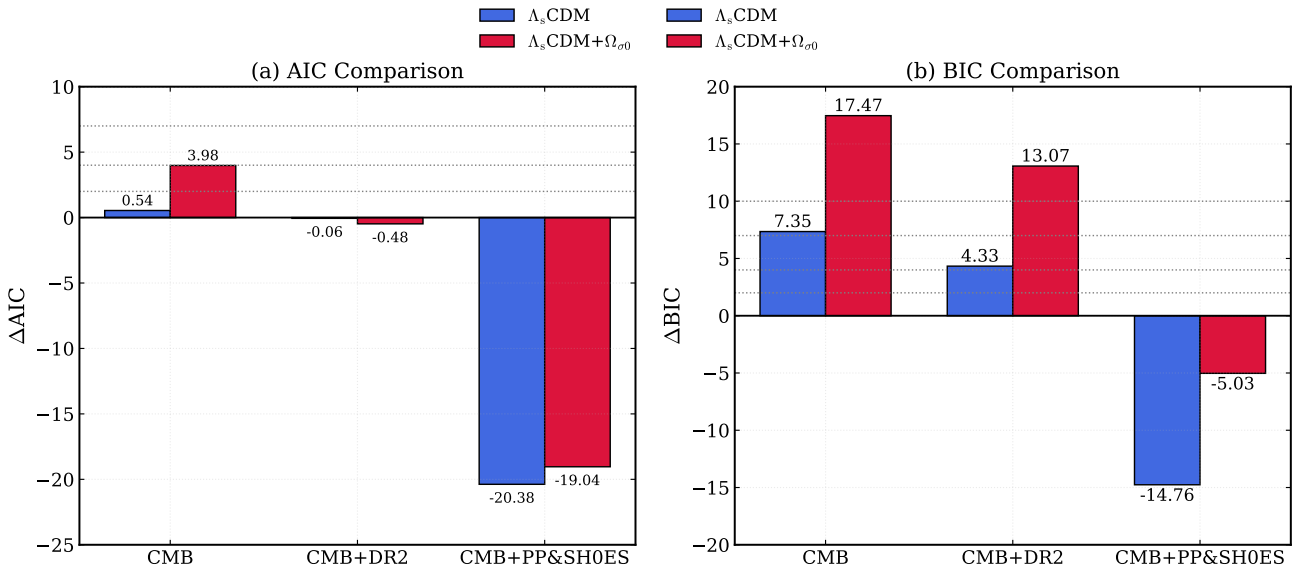


Figure 5: Statistical comparison all given cosmological models based on AIC and BIC from CMB, CMB+DR2 and CMB+PP&SH0ES datasets.

of data points N and the additional free parameters present in our model compared with ΛCDM. As discussed by Parkinson et al. (2005) (Parkinson et al., 2005) and Biesiada (2007) (Biesiada, 2007), for datasets with a large number of observations, such as CMB, and SNIa samples, AIC generally tends to favor models with more parameters owing to its weaker penalty term. In contrast, BIC imposes a stronger penalty on model complexity, thereby disfavoring models with additional parameters unless they provide a significantly improved fit. Many previous studies have found increased ΔAIC and ΔBIC

scores for extended cosmologies relative to the baseline ΛCDM framework (Yadav et al., 2026d; Xu & Zhang, 2016; Rezaei & Malekjani, 2021; Xincheng et al., 2024; Dixit et al., 2025).

5 Conclusion

In this study, we investigated an anisotropic extension of sign-switching dark energy cosmology by introducing a shear contribution within the Bianchi type-I framework. This extended scenario, denoted as Λ_sCDM+$\Omega_{\sigma 0}$, enables us to explore the combined effects of anisotropic cosmic expansion and a dynamical cosmological constant that undergoes a sign transition during the evolution of the Universe.Using recent cosmological observations, including the CMB measurements, DESI DR2 BAO data, and the PantheonPlus&SH0ES Type Ia supernova compilation, we performed a comprehensive parameter estimation analysis based on the Markov Chain Monte Carlo technique. Our results indicate that the present-day anisotropy parameter is tightly constrained to extremely small values, $\Omega_{\sigma 0} \lesssim \mathcal{O}(10^{-16})$ at the 95% confidence level. This finding implies that any residual anisotropic expansion in the present universe is strongly suppressed and remains consistent with the current observational bounds derived from the CMB and large-scale structure measurements.

We also examined the transition redshift $z_\dagger$, which characterizes the epoch at which the cosmological constant switches its sign from negative values in the early universe to positive values at later times. The observational constraints indicate that the transition occurs at a moderately high redshift, with additional datasets improving the precision of the lower bound of $z_\dagger$. Our analysis further shows that the inclusion of anisotropy has only a minor effect on the preferred range of this parameter, suggesting that the sign-switching mechanism remains robust even in the presence of small anisotropic contributions. A notable outcome of our analysis is the Hubble constant. The Λ_sCDM+$\Omega_{\sigma 0}$ model predicts a higher central value of H_0 compared with the standard ΛCDM framework. In particular, the CMB+PP&SH0ES dataset combination yields $H_0 = 72.25 \pm 0.90$ km s^{-1} Mpc^{-1}, which is in good agreement with the local distance-ladder measurements. Consequently, the long-standing Hubble tension between early- and late-universe probes is reduced to approximately the 3.7σ level within this extended framework. In addition, the predicted values of clustering parameter S_8 remain consistent with recent weak-lensing observations, indicating that the model does not introduce significant discrepancies in the matter clustering amplitude. We conclude that the cosmological parameter constraints derived from the anisotropic Λ_sCDM+$\Omega_{\sigma 0}$ and isotropic Λ_sCDM sign-switch models remain nearly indistinguishable. A possible explanation is that the contribution of anisotropy becomes significant primarily at higher redshifts, whereas the impact of the sign-switch model diminishes significantly after the transition redshift. Consequently, the additional anisotropic contribution has only a slight influence on the overall cosmological evolution, leading to almost identical cosmological predictions in both models. To evaluate the statistical performance of the proposed model, we also performed a model comparison using the Akaike Information Criterion (AIC) and Bayesian Information Criterion (BIC). The results demonstrate that the Λ_sCDM+$\Omega_{\sigma 0}$ model is observationally competitive with, and in certain dataset combinations strongly favored over, the standard ΛCDM cosmology. In particular, the combination of CMB and supernova data provided strong statistical support for the extended model. Our analysis shows that incorporating a small anisotropic component within the sign-switching dark energy framework provides a consistent and observationally viable extension of the standard cosmological model. The proposed scenario not only preserves the successful predictions of ΛCDM at late times but also offers a potential pathway toward alleviating some of the current cosmological tensions. Future high-precision observations from future cosmological surveys will further test the viability of this framework and help clarify the possible role of anisotropic expansion in the evolution of the universe.

Acknowledgments

The authors (A. Dixit and A. Pradhan) are thankful to IUCAA, Pune, India for providing support and facilities under the Visiting Associateship program. M. Yadav was sponsored by a senior Research Fellowship from the Council of Scientific and Industrial Research, Government of India (CSIR/UGC Ref. No. 180010603050). The authors would like to thank Dr. Ashutosh Singh for his helpful conversation and ideas.

Author Contributions

MY: Writing-original draft, Programming, AD: Investigation, Writing-review, Editing. AP: Writing-review, Editing, Supervision. MSB: Conceptualization, Investigation.

Funding

There is no funding associated with this manuscript.

Ethics Declaration

Ethics declaration is not applicable.

Declaration of competing interest

The authors declare that they have no known competing financial interests or personal relationships that could have influenced the work reported in this study.

Data availability

We employed publicly available CMB, Pantheon Plus SH0ES, Cosmic Chronometer (CC), BBN and DESI-DR2 data presented in this study. The CC data were compiled from publicly available cosmic chronometer measurements in the literature, with a representative compilation available at: https://github.com/AhmadMehrabi Cosmic chronometer data. The CMB, Pantheon Plus SH0ES and BBN data compilation (distance moduli and covariance matrices), which is publicly available on GitHub: https://github.com/brinckmann/montepython/public/tree/3.6/montepython/likelihoods and the DESI-DR2 data which is publicly available on Github: https://github.com/LauraHerold/MontePython/desilike/blob/main/likelihood/bao_desi_all/ . No additional data were used in this study.

References

Abbott, T.M.C., et al. [DES Collaboration]: Dark Energy Survey Year 3 results: Cosmological constraints from galaxy clustering and weak lensing. Phys. Rev. D **105**, 023520 (2022)

Abbott, T.M.C., et al.,: DES Y3 + KiDS-1000: consistent cosmology combining cosmic shear surveys. Open J. Astrophys. 6. (2023).

Abdul Karim, M., et al.: DESI DR2 results. II. Measurements of baryon acoustic oscillations and cosmological constraints, Phys. Rev. D **112**, 083515 (2025)

Ade, P.A.R. et al.: Planck 2015 results. XIII. Cosmological parameters, Astron. Astrophys. **594**, A13 (2016)

Aghanim, N., et al. [Planck Collaboration]: Planck 2018 results. VI. Cosmological parameters, Astron. Astrophys. **641**, A6 (2020)

Akaike, H.: A new look at the statistical model identification, IEEE transactions on automatic control. **19**, 716 (1974)

Akarsu, Ö., Barrow, J.D, Escamilla, L.A., Vazquez, J.A.: Graduated dark energy: Observational hints of a spontaneous sign switch in the cosmological constant. Phys. Rev. D **101**, 063528 (2020)

Akarsu, Ö., Barrow, J.D., Uzun, N.M.: Screening anisotropy via energy-momentum squared gravity: ΛCDM model with hidden anisotropy. Phys. Rev. D **102**, 124059 (2020)

Akarsu, Ö., Bulduk, B., De Felice, A., Katırcı, N., Uzun, N.M.: Unexplored regions in teleparallel $f(T)$ gravity: Sign-changing dark energy density, Phys. Rev. D **112**, 083532 (2025)

Akarsu, Ö., et al.: $\Lambda_{\rm s}$CDM cosmology from a type-II minimally modified gravity. Mon. Not. Roy. Astron. Soc. **546**, 1 (2026a).

Akarsu, Ö., De Valentino, E., Vyskočil, J., Yılmaz, E., Yükselci, A.E., Zhuk, A.: Nonlinear Matter Power Spectrum from relativistic N-body Simulations: Λ_sCDM versus ΛCDM. Phys. Rev. D **113**, 083508 (2026b)

Akarsu, Ö., Di Valentino, E., Kumar, S., Özyiğit, M., Sharma, S.: Testing spatial curvature and anisotropic expansion on top of the ΛCDM model, Phys. Dark Univ. **39**, 101162 (2023a)

Akarsu, Ö., Di Valentino, E., Kumar, S., Nunes, R.C., Vazquez, J.A., Yadav, A.: $\Lambda_{\rm s}$CDM model: A promising scenario for alleviation of cosmological tensions, arXiv:2307.10899 (2023b).

Akarsu, Ö., Kumar, S., Özülker, E., Vazquez, J.A., Yadav, A.: Relaxing cosmological tensions with a sign switching cosmological constant: Improved results with Planck, BAO, and Pantheon data. Phys. Rev. D **108**, 023513 (2023c).

Akarsu, Ö., Katırcı, N., Özdemir, N., Vázquez, J.A.: Anisotropic massive Brans-Dicke gravity extension of the standard ΛCDM model, Eur. Phys. J. C **80**, 32 (2020)

Akarsu, Ö., Kumar, S., Özülker, E., Vazquez, J.A.: Relaxing cosmological tensions with a sign switching cosmological constant. Phys. Rev. D **104**, 123512 (2021)

Akarsu, Ö., Kumar, S., Sharma, S., Tedesco, L.: Constraints on Bianchi type-I spacetime extension of the standard ΛCDM model, Phys. Rev. D **100**, 023532 (2019)

Alam, S., et al. [eBOSS Collaboration]: Completed SDSS-IV extended Baryon Oscillation Spectroscopic Survey: Cosmological implications from two decades of spectroscopic surveys at the Apache Point Observatory. Phys. Rev. D **103**, 083533 (2021)

Almeida, J.P.B., Guarnizo, A., Kase, R., Tsujikawa S., Valenzuela-Toledo, C.A.: Anisotropic 2-form dark energy. Phys. Lett. B **793**, 396 (2019)

Amirhashchi, H., Amirhashchi, S.: Constraining Bianchi Type I universe with Type Ia supernova and $H(z)$ data, Phys. Dark Univ. **29**, 100557 (2020).

Amirhashchi, H.: Probing dark energy in the scope of a Bianchi type I spacetime, Phys. Rev. D **97**, 063515 (2018)

Amirhashchi, H., Amirhashchi, S.: Current constraints on anisotropic and isotropic dark energy models. Phys. Rev. D **99**, 023516 (2019)

Amon, A., et al. (DES Collaboration): Dark Energy Survey Year 3 results: Cosmology from cosmic shear and robustness to data calibration. Phys. Rev. D 105, 023514 (2022)

Asgari, M., et al.: Kids-1000 cosmology: cosmic shear constraints and comparison between two point statistics. Astron. Astrophys. 645, A104 (2021)

Asvesta, K., Kazantzidis, L., Perivolaropoulos, L., Tsagas, C.G.: Observational constraints on the deceleration parameter in a tilted universe. Mon. Not. Roy. Astron. Soc. **513**, 2394 (2022)

Audren, B., Lesgourgues, J., Benabed, K., Prunet, S.: Conservative constraints on early cosmology with MONTE PYTHON. JCAP **001**, 02 (2013).

Barrow, J.D.: Cosmological limits on slightly skew stresses. Phys. Rev. D **55**, 7451 (1997)

Bhardwaj, V.K., Dixit, A., Rani, R., Goswami, G.K., Pradhan, A.: An axially symmetric transitioning models with observational constraints. Chin. J. Phys. **80**, 261–274 (2022)

Biesiada, M.: Information criteria and cosmological model selection. Phys. Rev. D **76**, 103514 (2007)

Breuval, L., et al.: Small Magellanic Cloud Cepheids observed with the Hubble Space Telescope provide a new anchor for the SH0ES distance ladder, Astrophys. J. **973**, 30 (2024)

Brinckmann, T., Lesgourgues, J.: MontePython 3: Boosted MCMC sampler and other features, Phys. Dark Univ. **24**, 100260 (2019).

Borkar, M.S., Charjan, S.S.: Bianchi type I magnetized cosmological model in bimetric theory of gravitation. Appl. Appl. Math. **5**, 23 (2010)

Boubel, P., Colless, M., Said, K., Staveley-Smith, L.: Testing anisotropic Hubble expansion, J. Cosmol. Astropart. Phys. **2025**(03), 066 (2025).

Bouhmadi-López, M., Ibarra-Uriondo, B.: Cosmographic analysis of sign-switching dark energy, Phys. Rev. D **112**, 063559 (2025a).

Bouhmadi-López, M., Ibarra-Uriondo, B.: Cosmological perturbations for smooth sign-switching dark energy models. Phys. Dark Univ. **50**, 102129 (2025b).

Camarena D., Marra, V., Sakr, Z., Clarkson, C.: A void in the Hubble tension? The end of the line for the Hubble bubble. Class. Quant. Grav. **39**, 184001 (2022)

Campanelli, L., Cea, P., Fogli, G.L., Marrone, A.: Testing the isotropy of the Universe with type Ia supernovae. Phys. Rev. D **83**, 103503 (2011)

Campanelli, L., Cea, P., Tedesco, L.: Cosmic microwave background quadrupole and ellipsoidal Universe. Phys. Rev. D **76**, 063007 (2007)

Camphuis, E., et al.: SPT-3G D1: CMB temperature and polarization power spectra and cosmology from 2019 and 2020 observations of the SPT-3G Main field, arXiv:2506.20707 (2025)

Chang, Z., Lin, H.N., Sang, Y., Wang, S.: A tomographic test of cosmological principle using the JLA compilation of type Ia supernovae, Mon. Not. Roy. Astron. Soc. **478**, 3633 (2018)

Chen, Y., Kumar, S., Ratra, B., Xu, T.: Effects of Type Ia supernovae absolute magnitude priors on the Hubble constant value. Astrophys. J. Lett. **964**, L4 (2024).

Colin, J., Mohayaee, R., Sarkar, S., Shafieloo, A.: Probing the anisotropic local Universe and beyond with SNe Ia data. Mon. Not. Roy. Astron. Soc. **414**, 264 (2011)

Dalal, R., et al.: Hyper suprime-cam year 3 results: cosmology from cosmic shear power spectra. Phys. Rev. D 108, 123519 (2023)

Dixit, A., Maurya, D.C., Pradhan, A.: Phantom dark energy nature of bulk-viscosity universe in modified $f(Q)$ gravity, Int. J. Geom. Methods Mod. Phys. **19**, 2250198 (2022)

Dixit, A., Pradhan, A., Bhardwaj, V.K., Beesham, A.: Observational constraints for an axially symmetric transitioning model with bulk viscosity parameterization, Astron. Comput. **45**, 100768 (2023)

Dixit, A., Yadav, M., Pradhan, A., Barak, M.S.: Beyond ΛCDM: Exploring a dynamical cosmological constant framework consistent with late-time observations, Ann. Phys. **483**, 170275 (2025)

Esposito, F., Carloni, S., Vignolo, S.: Bianchi type-I cosmological dynamics in $f(\mathcal{Q})$ gravity: a covariant approach. arXiv:2207.14576 (2022)

Faraoni, V., Coté, J.: Imperfect fluid description of modified gravities, Phys. Rev. D **98**, 084019 (2018)

Fayaz, V., Hossienkhani, H., Pasqua, A., Amirabadi, M., Ganji, M.: $f(T)$ theories from holographic dark energy models within Bianchi type I universe, Eur. Phys. J. Plus **130**, 28 (2015)

Gelman, A., Rubin, D.B.: Inference from iterative simulation using multiple sequences. Stat. Sci. **7** 472 (1992)

Heinesen A., Macpherson, H.J.: A prediction for anisotropies in the nearby Hubble flow, JCAP **03**, 057 (2022)

Hu, J.P., Wang, Y.Y., Wang, F.Y.: Testing cosmic anisotropy with Pantheon sample and quasars at high redshifts Astron. Astrophys. **643**, A93 (2020)

Jimenez, J. B., Salzano, V., Lazkoz, R.: Anisotropic expansion and SNIa: An open issue, Phys. Lett. B **741**, 168 (2015)

Kalus, B., Schwarz, D.J., Seikel, M., Wiegand, A.: Constraints on anisotropic cosmic expansion from supernovae. Astron. Astrophys. **553**, A56 (2013)

Kibaroğlu, S., Senay, M.: Anisotropic cosmology in q-deformed entropic gravity, Nucl. Phys. B **1012**, 116820 (2025).

Krishnan, C., Mohayaee, R., Colgáin, E. Ó, Sheikh-Jabbari, M.M., Yin, L.: Hints of FLRW breakdown from supernovae, Phys. Rev. D **105**, 063514 (2022)

Kogut, A., Hinshaw, G., Banday, A.J.: Limits to global rotation and shear from the COBE DMR four-year sky maps. Phys. Rev. D **55**, 1901 (1997)

Koussour, M., S. H. Shekh, S.H., and M. Bennai, M.: Bianchi type-I Barrow holographic dark energy model in symmetric teleparallel gravity. Int. J. Mod. Phys. A **37**, 2250184 (2022)

Koivisto, T., Mota, D.F.: Accelerating cosmologies with an anisotropic equation of state, Astrophys. J. **679**, 1 (2008)

Lewis, A.: GetDist: a python package for analysing Monte Carlo samples, arXiv:1910.13970 [astro-ph.IM] (2019)

Lin, H.N., Wang, S., Chang, Z., Li, X.: Testing the isotropy of the Universe by using the JLA compilation of type-Ia supernovae. Mon. Not. Roy. Astron. Soc. **456**, 1881 (2016)

Li, X., Lin, H.N., Wang, S., Chang, Z.: A unified description for dipoles of the fine-structure constant and SnIa Hubble diagram in Finslerian universe., Eur. Phys. J. C **75**, 181 (2015)

Luongo, O., Muccino, M., Colgáin, E. Ó., Sheikh-Jabbari, M.M., Yin, L.: Larger H_0 values in the CMB dipole direction. Phys. Rev. D **105**, 103510 (2022)

Macpherson, H.J., Heinesen, A.: Luminosity distance and anisotropic sky-sampling at low redshifts: A numerical relativity study, Phys. Rev. D **104**, 023525 (2021) [erratum: Phys. Rev. D **104**, 109901 (2021)]

Mandal, S.: Observational constraints on new class dark energy parameterized EoS in Bianchi type-I universe, J. High Energy Astrophys. **52**, 100564 (2026)

Martinez-Gonzalez, E., Sanz, J.L.: $\delta T/T$ and the isotropy of the Universe, Astron. Astrophys. **300**, 346 (1995)

Migkas, K., et al.: Probing cosmic isotropy with a new X-ray galaxy cluster sample through the L_X-T scaling relation. Astron. Astrophys. **636**, A15 (2020)

Migkas, K., et al.: Cosmological implications of the anisotropy of ten galaxy cluster scaling relations. Astron. Astrophys. **649**, A151 (2021)

Mimoso J.P., Wands, D.: Anisotropic scalar-tensor cosmologies. Phys. Rev. D **52**, 5612 (1995)

Montani, G., Escamilla, L.A., Carlevaro, N., Di Valentino, E.: Decay of $f(R)$ quintessence into dark matter: Mitigating the Hubble tension? Phys. Rev. D **113**, 023507 (2026).

Mule, L.R., Gaikwad, S.P., Mete, V.G.: Bianchi type-III holographic dark energy cosmological model in $f(R,T)$ theory of gravitation. New Astron. **105**, 102087 (2024)

Palacios-Córdoba, J.L., Orjuela-Quintana, J.B., Valencia-Zuñiga, G.A. Valenzuela-Toledo, C.A.: Anisotropic universes in light of background cosmological observations. Phys. Rev. D **113**, 043511 (2026)

Paliathanasis, A.: Anisotropic spacetimes in $f(T,B)$ theory I: Bianchi I universe, Eur. Phys. J. Plus **137**, 1 (2022)

Park, C.G., Ratra, B.: Using the tilted flat-ΛCDM and the untilted non-flat ΛCDM inflation models to measure cosmological parameters from a compilation of observational data, Astrophys. J. **882**, 158 (2019)

Park, C.G., Ratra, B.: Using SPT polarization, Planck 2015, and non-CMB data to constrain tilted spatially-flat and untilted nonflat ΛCDM, XCDM, and ϕCDM dark energy inflation cosmologies, Phys. Rev. D **101**, 083508 (2020).

Parkinson, D., Bassett, B.A., Barrow, J.D.C.: Model selection and the dark energy equation of state. Phys. Rev. D **72**, 083525 (2005).

Perlmutter, S., et al. [Supernova Cosmology Project]: Measurements of Ω and Λ from 42 high redshift supernovae, Astrophys. J. **517**, 565 (1999)

Pradhan, A., Dixit, A., Varshney, G.: LRS Bianchi type-I cosmological models with periodic time varying deceleration parameter in $f(R,T)$ gravity, Int. J. Mod. Phys. A **37**, 2250121 (2022)

Rahman, W., Trotta, R., Boruah, S.S., Hudson, M.J., van Dyk, D.A., New constraints on anisotropic expansion from supernovae Type Ia, Mon. Not. Roy. Astron. Soc. **514**, 139 (2022)

Rezaei, M., Malekjani, M.: Comparison between different methods of model selection in cosmology, Eur. Phys. J. Plus **136**, 219 (2021)

Riess, A.G., et al. [Supernova Search Team]: Observational evidence from supernovae for an accelerating universe and a cosmological constant, Astron. J. **116**, 1009 (1998)

Riess, A.G., et al.: A comprehensive measurement of the local value of the Hubble constant with uncertainty from the Hubble Space Telescope and the SH0ES team, Astrophys. J. Lett. **934**, L7 (2022)

Saadeh, D., Feeney, S.M., Pontzen, A., Peiris, H.V., McEwen, J.D.: How Isotropic is the Universe? Phys. Rev. Lett. **117**, 131302 (2016a)

Saadeh, D., Feeney, S.M., Pontzen, A., Peiris, H.V., McEwen, J.D.: A framework for testing isotropy with the cosmic microwave background, Mon. Not. Roy. Astron. Soc. **462**, 1802 (2016b).

Santhi, M.V., Chinnappalanaidu, T.: Tsallis holographic dark energy in Bianchi type-II, VIII and IX universes. Astrophys. Space Sci. **368**, 32 (2023)

Schwarz, G.E.: Estimating the dimension of a model. Ann. Statist. **6**, 461 (1978)

Scolnic, D., Brout, D., et al.: The Pantheon+ Analysis: The Full Data Set and Light-curve Release. Astrophys. J. **938**, 113 (2022)

Secrest, N.J., von Hausegger, S., Rameez, M., Mohayaee, R., Sarkar, S., Colin, J.: A test of the cosmological principle with quasars. Astrophys. J. Lett. **908**, L51 (2021)

Siewert, T.M., Schmidt-Rubart, M., Schwarz, D.J.: Cosmic radio dipole: Estimators and frequency dependence. Astron. Astrophys. **653**, A9 (2021)

Singh, A.: Homogeneous and anisotropic cosmologies with affine EoS: a dynamical system perspective, Eur. Phys. J. C **83**, 696 (2023)

Singh, A. et al.: Observational constraints on the expansion scalar and shear relation in the Locally rotationally symmetric Bianchi I model, Phys. Dark Uni. **47**, 101798 (2025)

Singh, A., Krishnannair, S.: The dark sector coupling in anisotropic model: observational aspects and cosmic dynamics, Gen. Relativ. Gravit., **58**, 89 (2026)

Singha, R., Singh, A.: An observational study of the affine EoS cosmological model, Indian J. Phys. **100**, 1247–1259 (2026)

Solanke, Y.S., Kale, A.P., Pawar, D.D., Dagwal, V.J.: LRS Bianchi type-I cosmological model in $f(Q,T)$ theory of gravity with observational constraints. Int. J. Geom. Methods Mod. Phys. **20**, 2350212 (2023)

Soltis, J., Farahi, A., Huterer, D., Liberato, C.M.: Percent-Level Test of Isotropic Expansion Using Type Ia Supernovae. Phys. Rev. Lett. **122**, 091301 (2019)

Valentino, E. Di., et al.: Snowmass2021 - Letter of interest cosmology intertwined II: The Hubble constant tension. Astropart. Phys. **131**, 102605 (2021)

Valentino, E.Di, Said, J.E., Network, T.C.L.: The CosmoVerse White Paper: Addressing observational tensions in cosmology with systematics and fundamental physics. Phys. Dark Univ. **49**, 101965 (2025)

Verma, S., Dixit, A., Pradhan, A., Barak, M.S.: Testing $f(T)$ gravity with cosmological observations: Confronting the Hubble tension and implications for the late-time universe. J. High Energy Astrophys. **49**, 100440 (2026)

Vinutha T., Kavya, K.S.: The study of Bianchi type-III, V, and VI_0 models in modified theory. Int. J. Geom. Methods Mod. Phys. **19**, 2250046 (2022)

Wang, Y.Y., Wang, F.Y.: Testing the isotropy of the Universe with type Ia supernovae in a model-independent way. Mon. Not. R. Astron. Soc. **474**, 3516 (2018)

Wilczynska, M.R., et al.: Four direct measurements of the fine-structure constant 13 billion years ago,. Sci. Adv. **6**, eaay9672 (2020)

Wright, A.H., et al.: KiDS-Legacy: cosmological constraints from cosmic shear with the complete Kilo-Degree Survey. Astron. Astrophys. 703, A158 (2025).

Xu, Y.Y., Zhang, X.: Comparison of dark energy models after Planck 2015. Eur. Phys. J. C **76**, 588 (2016)

Xincheng, Z., Xu, R., Xu, D.: Bumblebee cosmology: Tests using distance-and time-redshift probes. arXiv preprint arXiv:2411.18559 (2024)

Yadav, V.: Measuring Hubble constant in an anisotropic extension of ΛCDM model. Phys. Dark Univ. **42**, 101365 (2023)

Yadav, V., Rajpal, Pardeep, Yadav, M., Yadav, S.K.: Testing spatial curvature in an anisotropic extension of wCDM model with low redshift data. arXiv:2405.11534 (2024)

Yadav, A., Kumar, S., Kibris, C., Ozgur Akarsu. O.: Λ_sCDM cosmology: Alleviating major cosmological tensions by predicting standard neutrino properties. JCAP **2025(01)**, 042 (2025a)

Yadav, M., Dixit, Barak, M.S., Pradhan, A.: Investigating the wCDM model with latest DESI BAO observations. Eur. Phys. J. C **85**, 1013 (2025b)

Yadav, M., Dixit, A., Pradhan, A., Barak, M.S.: Cosmological implications of a new creation field in Hoyle–Narlikar gravity with bulk viscous fluid. arXiv:2509.19356[gr-qc] (2025c)

Yadav, M., Dixit, A., Pradhan, A., Barak, M.S.: Empirical validation: Investigating the ΛsCDM model with new DESI BAO observations, J. High Energy Astrophys. **49**, 100453 (2026a).

Yadav, M., Dixit, A., Barak, M.S., Pradhan, A.: Constraints on spatial curvature and dark energy dynamics in the wCDM model from DESI DR1 and DR2, J. High Energy Astrophys. **50**, 100514 (2026b)

Yadav, M., Dixit, A., Barak, M.S., Pradhan, A.: Dynamical oscillations in dark energy: Joint constraints on the $w_{\sin}$CDM model from DESI, OHD, and supernova samples. J. High Energy Astrophys. **51**, 100556 (2026c)

Yadav, M., Dixit, A., Pradhan, A., Barak, M.S.: A new creation-field cosmology in Hoyle–Narlikar gravity: Dark energy dynamics, cosmic acceleration, and the Hubble tension. Int. J. Geom. Methods Mod. Phys. 2650373 (2026d), https://doi.org/10.1142/S0219887826501471

Yadav, M., Dixit, A., Pradhan, A., Barak, M.S.: Dynamical dark energy signatures from a new transition $Om(z)$ parametrization in flat FLRW cosmology. Phys. Lett. B **874**, 140238 (2026d)

Yeung, S., Chu, M.C.: Directional variations of cosmological parameters from the Planck CMB data. Phys. Rev. D **105**, 083508 (2022)

Zhao, D., Zhou, Y., Chang, Z. Anisotropy of the Universe via the Pantheon supernovae sample revisited. Mon. Not. R. Astron. Soc. **486**, 5679 (2019)